



Influence of Zn(II) stress-induction on component variation and sorption performance of extracellular polymeric substances (EPS) from *Bacillus vallismortis*

Peifei Ding¹ · Weifeng Song¹ · Ziheng Yang¹ · Jingyi Jian²

Received: 21 December 2017 / Accepted: 11 February 2018 / Published online: 17 February 2018
© Springer-Verlag GmbH Germany, part of Springer Nature 2018

Abstract

Bacillus vallismortis (*B. vallismortis*), an aerobic heterotrophic bacteria, was screened in a laboratory pilot study, to assess the interaction between the heavy metal Zn(II) and extracellular polymeric substances (EPS). The influence of Zn(II) stress on EPS production, component variation, and sorption performance, was investigated. The characteristics of *B. vallismortis* EPS formed under stress were analyzed using FTIR, 3D-EEM and XPS. EPS was used as an adsorbent and the adsorption capacity and adsorption behavior of EPS formed with and without Zn(II) stress, were compared and assessed. Results showed that the production of polysaccharides and proteins, the main components of EPS, were promoted under Zn(II) stress. The types of EPS functional groups observed remained the same with and without heavy metal stress, but their concentrations were increased. Due to stress-induction, the adsorption capacity of Zn-EPS was significantly enhanced compared with the control-EPS. Specific EPS produced by *B. vallismortis* in the presence of Zn(II) stress, could have a wide range of potential applications, allowing optimization and improvement of the capacity of EPS to remove heavy metals from effluent.

Keywords Stress/induction · Heavy metals · Extracellular polymeric substances · Characteristic · Adsorption

Introduction

Heavy metals are generally toxic to biological systems and non-biodegradable. The uptake and accumulation of heavy metals damage the metabolic activity of organisms, posing a risk to the natural environment and human health. Therefore, the issue of how to efficiently deal with heavy metal-containing wastewaters is a significant problem in the field of environmental science, that has received much research attention. Conventional methods used for removing heavy metal ions from wastewater include chemical precipitation, filtration, chemical reduction, and ion exchange. However, physico-chemical processes

such as these may be ineffective when initial heavy metal concentrations are low [1]. The use of microorganisms in biosorption systems has been extensively studied due to their potential environmentally friendly and cost-effective applications, as well as their high heavy metals removal efficiency [2]. In addition, in recent years the huge potential of extracellular polymeric substances (EPS) produced by biomass cell walls, has been established and received notable research attention.

EPS comprises polysaccharides, proteins, nucleic acids and lipids. It is negatively charged due to the dominance of carboxy and hydroxyl functional groups, which are also known to be involved in metal binding processes and facilitates adsorption [3]. Many researches mainly focused on the influence and the mechanism of microbial removal of heavy metals by EPS. Deschatre et al. [4] proposed that the functional groups involved in metal adsorption are $-\text{COOH}$, $-\text{NH}_2$, $-\text{CH}_2-$, $-\text{OH}$ and $-\text{C}=\text{O}$, with ion exchange and complexation being the main adsorption mechanisms. Nevertheless, the effects of heavy metals on EPS and its interactions, have not received in-depth assessment. Various studies on

✉ Weifeng Song
weifengsong@gdut.edu.cn

¹ College of Environmental Science and Engineering,
Guangdong University of Technology, Guangzhou 510006,
People's Republic of China

² Environmental Technology Center of Panyu District,
Guangzhou 511499, People's Republic of China

bacterial EPS under metal stress conditions have been reported in recent years [5–7], with the addition of heavy metals providing a stress factor as well as a removal target, with the effects of metal stress on EPS characteristics often obscured by physical adsorption. Therefore, investigating the effects of heavy metal stress on the characteristics and adsorption performance of EPS is essential, allowing wastewater treatment systems to promote microbes that produce specific EPS types and therefore improve their biosorption capability.

The refractory organic floatation reagent aniline aerofloat is a widely used collector in zinc containing wastewater from mining [8], as well as industrial wastewater containing organic contaminants and heavy metals. However, it does not break down easily and has a long residual life, consequently harming all living creatures and the human body. Therefore, the interaction between heavy metals and microorganism must be understood and optimized, for effective wastewater treatment.

In the current study, an aniline aerofloat strain, *Bacillus vallismortis* was applied. The production of EPS under Zn(II) stress and its adsorption capacities for heavy metals, were investigated. EPS was characterized in the presence or absence of Zn(II), using 3D-EEM, FTIR and XPS. The results provide new insights into the mechanism of interaction between EPS and heavy metals such as Zn(II). In addition, a feasible scheme for heavy metal removal is proposed, using specific EPS produced under heavy metal stress conditions.

Materials and methods

Bacterial activation and stress cultivation

The bacterial strain *B. vallismortis* was obtained from the School of Environmental Science and Engineering, Guangdong University of Technology (China). It was selected and isolated from flotation wastewater due to its capacity to degrade aniline aerofloat.

The strain *B. vallismortis* was activated from the aniline aerofloat culture by inoculating 250 mL flasks containing 0.1 g L⁻¹ aniline aerofloat, 1.6 g L⁻¹ KH₂PO₄, 0.4 g L⁻¹ K₂HPO₄, 0.06 g L⁻¹ MgSO₄, 0.001 g L⁻¹ CaCl₂ and 1.0 g L⁻¹ NH₄Cl. It was cultivated at 35 °C in a temperature-controlled THZ-98C shaking incubator (Shanghai Yihen Scientific Instruments Co. Ltd., Shanghai, China) at a shaking speed of 150 rpm for 48 h.

Zn(II) in form of ZnSO₄ was added to Luria broth medium (10.0 g L⁻¹ peptone, 5.0 g L⁻¹ yeast extract, 10.0 g L⁻¹ NaCl) to the desired concentrations (depending on the strength of the stress), with a culture prepared

without the addition of heavy metals as the control. After activation, seed cultures were grown in 250 mL flasks containing Luria–Bertani medium with or without the addition of Zn(II) at 35 °C, with continual agitation at 150 rpm for 24 h.

EPS extraction and analysis

EPS production was monitored in a Luria–Bertani medium in the presence or absence of zinc sulfate, at varying concentrations, to assess the stress effect of zinc on EPS production. When cultures reached the stationary growth phase, they were harvested separately at 4000 rpm at 4 °C for 15 min. Supernatants were discarded, with the precipitate dissolved in sterile distilled water (prepared in the laboratory). This process was performed three times, with the final precipitate resuspended in a solution of 2% (V/V) disodium ethylenediaminetetraacetic acid (EDTA)-NaCl and then heated at 50 °C for 3 min. The EPS fraction was harvested at 10,000 rpm for 15 min at 4 °C, with the supernatant then filtered through a 0.22 μm cellulose nitrate filter, with the crude EPS filtrate then dialyzed for 24 h using distilled water to obtain pure EPS.

Polysaccharides and proteins were measured using the Anthrone colorimetric method [9] and Coomassie light blue method [10], while nucleic acids were measured using the diphenylamine method [11]. Total EPS was calculated as the sum of the three components and all tests were conducted in triplicate.

Zn(II) adsorption experiments

An adsorption experiment was designed to provide a quantitative characterization of Zn(II) binding by EPS, in the presence and absence of stress induced by varying metal ion concentrations. Bio-adsorption experiments were performed in a rotary shaker, with continual agitation at 150 rpm and at 35 °C in 250 mL flasks containing 20 mL ZnSO₄ solution (20 mg L⁻¹). The initial pH value of the solution was adjusted with 0.5 M H₂SO₄ and 0.5 M NaOH to pH 5. Different amounts of EPS formed in the presence or absence of stress was added to each flask. After shaking the flasks for 4 h, the reaction mixture was dialyzed for 12 h, with metal ions in the dialysate then measured using atomic adsorption spectrometry (HITACHI Z2000, Hitachi Limited, Tokyo, Japan). An equal volume of distilled water was used as the control, instead of EPS. Each exposure was performed in triplicate, with mean values used in the analysis of data.

Data evaluation

The quantity of metal ions adsorbed by EPS was calculated according to the initial concentration and equilibrium

concentration of metal ions, the volume of solution and EPS mass, using Eq. (1) as follows:

$$Q = \frac{C_0 V_0 - C_t V_t}{m} \quad (1)$$

where Q (mg g^{-1}) represents the metal adsorption quantity; C_0 and C_t (mg L^{-1}) are the initial and equilibrium concentrations of metallic ions, respectively; V_0 and V_t (L) are the initial and final volumes of solution, respectively; and m (g) is the mass of EPS.

Fluorescence EEM determination

Fluorescence EEM spectra were obtained using a HITACHI F4600 (Hitachi Limited, Tokyo, Japan) fluorescence spectrometer in scan mode, with a 700-V xenon lamp at room temperature. EEM spectra were established using scanning emission (Em), by varying the excitation (Ex) wavelength from 200 to 500 nm using 5 nm increments, with spectra recorded at a scan rate of 1200 nm min^{-1} , using Ex and Em slit widths of 5 nm. 3D-EEM data were processed using Origin 8.0 software.

Preparation of EPS samples

Cold ethanol was added to the EPS samples formed in the presence or absence of zinc stress at a volumetric ratio of 5:1 to precipitate the EPS content. The mixture was then stored at -18°C for 12 h and the final precipitate was separated from suspension in ethanol. EPS samples used for FTIR and XPS analysis were freeze-dried.

FTIR spectroscopy

FTIR spectra (Nicolet Avatar 380, Thermo Fisher Scientific, Waltham, MA, USA) using the KBr pressed disk technique were obtained using EPS produced by *B. vallismortis* in either presence or absence of Zn(II) stress.

XPS of EPS

XPS measurements were performed using an AXIS-ULTRA DLD (Shimadzu, Kyoto, Japan) Photoelectron Spectrometer with Al $K\alpha$ radiation. Survey spectra (0–1200 eV) were recorded at a pass energy of 100 eV, with 40 eV used for the detailed scans in the C 1 s, O 1 s and N 1 s regions. Binding energies were calibrated according to the C 1 s peak (284.8 eV). The software package XPSPEAK (4.01) was used to fit the XPS spectral peaks.

Adsorption isotherms

The adsorption capacity of the adsorbent mainly depends on the equilibrium concentration of metal adsorbates in solution. And the correlation between them is described by adsorption isotherms at a given temperature. There are several models for predicting the equilibrium distribution. However, the most commonly used isotherms for the application of heavy metal biosorption by EPS in solution are the Freundlich and Langmuir isotherms.

A. Langmuir model

The basic assumptions of Langmuir isotherm are as follows:

1. Monomolecular layer adsorption.
2. The surface is homogeneous.
3. Adsorption at one site does not affect the adjacent site.

To determine the maximum adsorption capacity for single metal solution, following equation is employed:

(Non-linear form)

$$Q_e = \frac{Q_m b C_e}{1 + b C_e} \quad (2)$$

(Linear form)

$$\frac{C_e}{Q_e} = \frac{1}{Q_m b} + \frac{C_e}{Q_m} \quad (3)$$

where C_e is the equilibrium concentration (mg L^{-1}), Q_e is the amount adsorbed per unit mass of adsorbent at equilibrium (mg g^{-1}). The Q_m and b are the Langmuir constants related to the adsorption capacity and energy of adsorption, respectively.

B. Freundlich model

This model is an empirical equation which considers the heterogeneity of the adsorbent surface:

$$Q_e = k C_e^{\frac{1}{n}} \quad (4)$$

Freundlich constants k and n related to adsorption capacity and intensity, respectively.

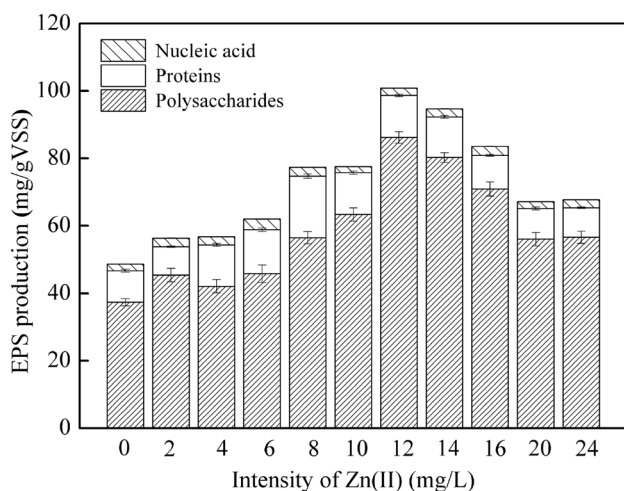


Fig. 1 EPS production by *B. vallismortis* and relative proportion of components, in response to exposure to varying concentrations of Zn(II)

Results and discussion

Effects of Zn(II) stress/induction intensity on EPS production and components

EPS production and component variation in response to varying Zn(II) concentrations are shown in Fig. 1, where it can be seen that Zn(II) had a significant effect on EPS produced by *B. vallismortis*. In the absence of Zn(II) (control-EPS), EPS concentrations were 48.65 mg g^{-1} VSS and consisted of 76.77% polysaccharides and 19.11% proteins, showing polysaccharides and proteins to be the major components of EPS. The production of EPS significantly increased with increasing concentrations of Zn(II). When the concentration of Zn(II) in the culture reached 12 mg L^{-1} , the production of the EPS reached its maximum concentration of 100.84 mg g^{-1} VSS, twofold that of the control-EPS. As shown in Fig. 1, the effect of Zn(II) on EPS production was significant within a certain Zn(II) concentration range. It is of note, that the concentration of polysaccharides and proteins did not increase in proportion with Zn(II) concentrations. When Zn(II) levels increased from 0 to 8 mg L^{-1} , the production of polysaccharides increased from 37.55 to 86.16 mg g^{-1} VSS, increasing the proportion of polysaccharides in total EPS from 76.77 to 85.44%. Similarly, with the increase in Zn(II), protein production increased from 9.30 to 18.29 mg g^{-1} VSS, showing an increase in the proportion of proteins in total EPS from 19.11 to 23.67%. These results show that the addition of Zn(II) to culture media, caused varying effects in EPS component abundance, with the changes in the polysaccharide fraction being more significant than the protein and nucleic acid fractions. This finding indicates that Zn(II)

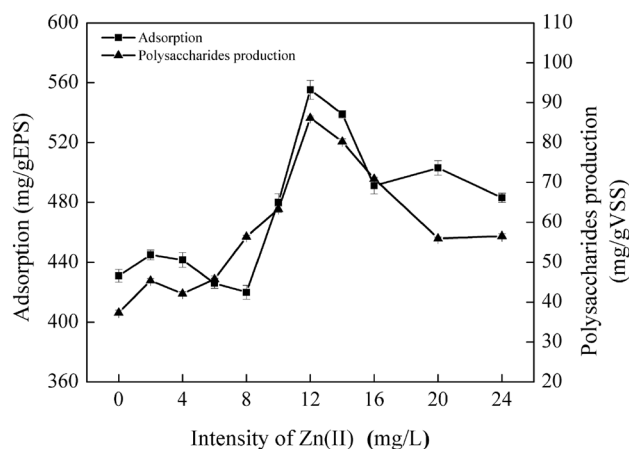


Fig. 2 Adsorption ability of EPS produced by *B. vallismortis* in response to varying concentrations of Zn(II)

exposure has a significant effect on the production of EPS polysaccharides, potentially due to Zn induced increases in the activity of glycogen synthase, promoting the polymerization of monosaccharides into polysaccharides due to glycosidic bond formation [12].

EPS is produced by bacteria for the purpose of adapting itself to varying external environments, such as increasing intensity of heavy metals, which induces adverse effects on bacteria. However, bacteria can increase their EPS production as a defense mechanism, in the presence of toxic metals, effectively increasing the viability of cells exposed to aqueous heavy metals [13]. EPS is a polymer which is synthesized and secreted due to various active enzymes and metabolic activities. Zinc is a necessary trace element for microbes, existing in the form of metal-containing enzyme proteins and having various significant roles in cell activities. Therefore, Zn exposure can improve the efficiency of enzymatic reactions and indirectly promote cell metabolism. Conversely, when Zn ions increase to higher concentrations, the production of EPS may decrease rapidly in bacteria, with bio-toxicity pathways being activated. The uptake and accumulation of heavy metals such as Zn, can cause various harmful effects at the cellular, physiological and molecular levels, including protein and DNA oxidation [14]. Heavy metal exposure can induce reactive oxygen species generation in cells [15, 16], with excess reactive oxygen species accumulating and resulting in enzyme inactivation and decreased EPS production [17, 18].

Metal adsorption of EPS

It is well established that heavy metals can easily bind to some functional groups such as carboxyl, amino and hydroxy groups. The different changes observed in the

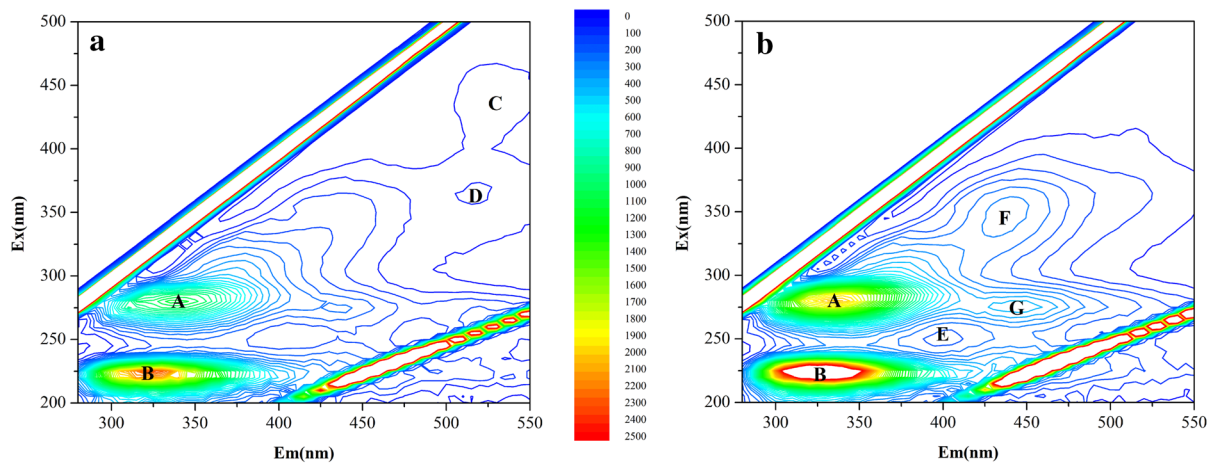


Fig. 3 3D-EEM of EPS produced by *B. vallismortis* in the presence or absence of Zn(II). **a** Control-EPS, **b** Zn-EPS

Table 1 Fluorescence spectra characteristics of EPS produced by *B. vallismortis* in the presence or absence of Zn(II)

Peak	Spectral peak information (Ex/Em, intensity)		Existing substances	References
	Control-EPS	Zn-EPS		
A	280/335, 1177	280/335, 2020	Tryptophan-like	[20]
B	225/320, 2372	225/325, 3394	Tyrosine-like	
C	441/525, 70.34	–	Fulvic-like	[22]
D	365/520, 106.4	–	Humus-like	[21]
E	–	250/401, 182.8	Humus-like	[23]
F	–	345/435, 321.2	Fulvic-like	[24]
G	–	275/446, 487.3	Fulvic-like	[21]

production of specific EPS components, due to the addition of Zn(II), may result in different relative concentrations of functional groups, which may affect Zn(II) adsorption by EPS. To confirm the adsorption performance of EPS produced in the presence and absence of Zn(II) stress, batch adsorption tests were performed and the results are shown in Fig. 2. Metal adsorption capacities of EPS showed no significant difference when the concentration of Zn(II) was below 8 mg L^{-1} , but increased from 430 to 555.27 mg g^{-1} EPS when Zn(II) concentrations increased to 12 mg L^{-1} , followed by a decrease in adsorption with further increases in concentration. The trends observed for both Zn adsorption and polysaccharides production showed high similarity over a wide range of Zn(II) concentrations. Naik et al. [19] found that EPS produced by *E. cloacae* strain P2B in the presence of lead nitrate, contained high concentrations of sugars containing hydroxyl groups, enabling EPS to become hydrated, swell and yield more viscous solutions, which can bind high levels of lead. Zinc has been reported to have a good binding affinity for hydroxyl groups of EPS polysaccharides [6], suggesting that the adsorption of Zn(II) is associated with EPS polysaccharides. Therefore, Zn(II) may stimulate *B. vallismortis* to

produce specific extracellular polysaccharides, containing active functional groups which could easily bind Zn(II), improving the adsorption capacity of EPS.

Effects of metal stress on EPS components

The results of 3D-EEM analysis of EPS produced in the presence (Zn-EPS) and absence (control-EPS) of stress are presented in Fig. 3. Four peaks can be observed in control-EPS, A, B, C and D, located at Ex/Em wavelengths of 280/335, 255/320–320, 441/525 and 365/520 nm, respectively. These peaks indicate that control-EPS was mainly composed of tryptophan—(peak A), tyrosine—(peak B), fulvic acid—(peak C) and humic acid-like substances—(peak D) [20, 21]. The fluorescence peak positions and EPS content were independent of each other, as shown in Fig. 3, although a close relationship was observed between fluorescent signal intensity and EPS content. The fluorescence peak positions of EPS produced in the presence and absence of stress, as well as the maximum fluorescence intensities, are presented in Table 1.

According to the results presented in Table 1 and Fig. 3, it may be concluded that the fluorescence intensity of peak

A and peak B increased under the stress of Zn(II), although their relative amplification was different. Peak A and peak B represent two kinds of proteins, which play important roles in the formation of aggregates and stabilizing structures, indicating that *B. vallismortis* could produce extracellular proteins containing tryptophan- and tyrosine-like substances. The presence of these proteins may help avoid heavy metal intracellular absorption, due to the binding and stabilization of metal ions, therefore, reducing toxicity to cells. In addition, peak E (Ex/Em of 250/401 nm), peak F (Ex/Em of 345/435 nm) and peak G (Ex/Em of 275/446 nm) were observed in Zn-EPS. Peak E and peak G represent humic acid- and fulvic acid-like substances, respectively [23], while peak F represents fulvic acid-like substances that are associated with carboxyl and carbonyl EPS groups. It is of note, that peak C and peak D disappeared under Zn(II) stress, showing that the stress of Zn(II) exposure altered EPS components produced, increasing the contents of protein-like substances which are essential in the binding of heavy metals [25].

Compared with control-EPS, peak B in Zn-EPS redshifted due to the increasing content of functional groups such as carboxyl, hydroxyl, amino and carbonyl groups [26, 27]. It has been established that a large number of negatively charged functional groups are key for effective binding of EPS to metal ions. The redshifting of Zn-EPS from the perspective of spectroscopy indicates that the chemical structures contained in EPS produced by *B. vallismortis*, changed according to Zn(II) stress. The abundance of negatively charged functional groups increased, resulting in enhancement of the capacity of binding of EPS and metal ions, therefore reducing the toxicity of Zn(II) to *B. vallismortis*.

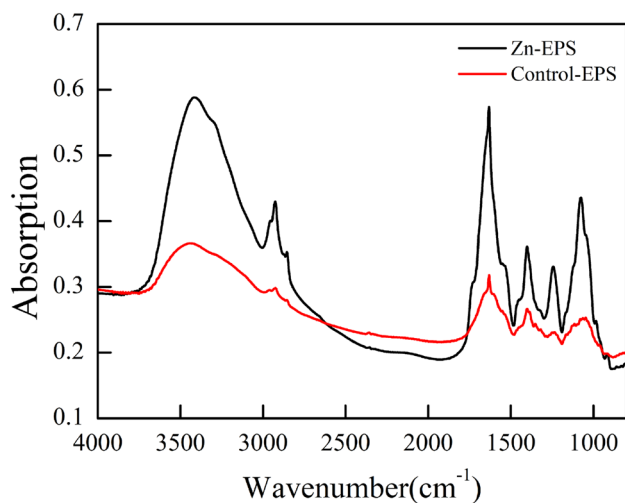


Fig. 4 FTIR spectrum of EPS produced by *B. vallismortis* in the presence or absence of Zn(II)

FTIR analysis of EPS

Identifying the functional groups present is one of the keys to understanding the mechanisms of EPS metal binding. Figure 4 shows FTIR spectra of EPS produced in the presence and absence of Zn(II) stress. Absorption peaks between 800 and 4000 cm^{-1} reveal that the components of EPS were complex and maintained the common microbial EPS composition, mainly including proteins and carbohydrates. According to published literature [28, 29], the bands observed at 3500–3400, 2960 and 1631 cm^{-1} corresponded to the hydroxyl group, $-\text{CH}_2-$ group and C=O component of Amide I, respectively; the peak at 1552 cm^{-1} corresponded to the N–H/C–H component of Amide II; the peaks observed at 1402 and 1240 cm^{-1} corresponded to carboxyl C=O and C–O, respectively. Polysaccharides groups ($-\text{OH}$ and C–O–C) were identified by vibrations at 1062 cm^{-1} , while bending at less than 1000 cm^{-1} represented fingerprint regions, mainly associated with sulphur and phosphorus groups of nucleic acids.

As can be seen from the infrared spectrogram (Fig. 4), the functional groups present in control-EPS and Zn-EPS showed no significant difference, containing hydroxyl, carboxyl and amide groups, C–O–C and lipids. This finding shows that metal stress did not affect the types of EPS functional groups observed, however, the shape and intensity of several characteristic peaks changed following Zn(II) stress. Jiang et al. [30] proposed a close relationship between peak intensity and the concentration of EPS functional groups. Xu et al. [31] studied the EPS of *B. cereus* using infrared spectra analysis, concluding that absorption peak intensity is positively correlated with the relative concentration of functional groups present. In the present study, the Zn-EPS absorption peak intensity was higher than that of control-EPS, indicating that the concentration of EPS functional groups was increased following Zn(II) stress, including C=O, C–O and $-\text{OH}$ in polysaccharides and C=O in proteins.

XPS analysis

Atomic fraction concentrations were examined by XPS, for both elements and functional groups present in EPS produced in the presence and absence of Zn(II). XPS spectra plot the number of electrons detected per unit of time versus the binding energy of electrons from the elements present in EPS. Each XPS spectrum peak corresponds to electrons with a characteristic binding energy from a particular element, with the peak intensity being proportional to the relative elemental abundance [32]. The examined EPS consisted of C, N and O, with these findings being consistent with results of infrared spectrum analysis. Compared with control-EPS, the relative content of C and N in Zn-EPS decreased by 4.46 and 1.23%, respectively, while the relative content of

Table 2 Content of three main components of EPS produced by *B. vallismortis*

Content	EPS	Zn-EPS
C_{PSs}/C	62.69	82.99
C_{PNs}/C	22.27	16.16
C_{Hc}/C	15.04	0.85

O increased by 5.69%. This finding indicates that *B. vallismortis* altered the produced EPS component under the stress of Zn(II) exposure, resulting in alteration to the relative elemental content.

The total EPS concentrations were estimated based on the three basic constituents, polysaccharides (PSs), proteins (PNs) and hydrocarbon-like products (Hc), using Eqs. (5), (6) and (7) as follows [33, 34]:

$$N/C = 0.279(C_{PNs}/C), \tag{5}$$

$$O/C = 0.325(C_{PNs}/C) + 0.833(C_{PSs}/C), \tag{6}$$

$$C/C = (C_{PNs}/C) + (C_{PSs}/C) + (C_{Hc}/C), \tag{7}$$

where O/C and N/C are the observed atomic concentration ratios of oxygen to carbon, or nitrogen to carbon, respectively, in the analyzed sample; while C_{PSs} , C_{PNs} and C_{Hc} are the atomic concentrations of carbon present in polysaccharides, proteins and hydrocarbon-like products, respectively.

Based on these equations, the proportion of carbon associated with each molecular constituent of control-EPS and Zn-EPS were converted to weight fractions and are listed in Table 2. The results show that polysaccharides represent the largest proportion of the three components in control-EPS, with the relative abundance of 62.69%. The observed protein content was less, with a relative abundance of 22.27%; while only a small proportion of hydrocarbons was observed. Following Zn(II) stress, the proportion of polysaccharides increased by more than 20%, while the proportion of proteins decreased by 6.11%. This finding indicates that the stress of Zn(II) exposure changed the elemental content and characteristics of EPS.

Carbon is one of the main elements contained in EPS and as presented in Table 3, the carbon peak can be deconvoluted

into four spectral regions [33, 35–37]. (1) Aliphatic C–C and C–H bonds (C–C, C–H); (2) carbon with a single bond to either oxygen or nitrogen (C–O, C–N), in the form of ether, ethanol or amine; (3) carbon with double bonds to oxygen, such as in ketones, esters or carboxyl groups (C=O, O=C–O); and (4) O–C–O or O=C–N bonds as observed in acetyl and amide groups. Compared with control-EPS, the C fraction of Zn-EPS belonging to C–C or C–H carbon bonds (peak 1) decreased by 16.35% and C–O or C–N carbon bonds decreased by 8.93%, whereas C=O or O=C–O carbon bonds and O–C–O or O=C–N carbon bonds increased by 3.05 and 22.23%, respectively. These results show that *B. vallismortis* combined C, O and N with oxygen to produce more carbon double bonds and amides, when under Zn(II) stress, allowing easier binding to metal ions. The decrease in C–C and C–H bonds, as well as the increase in oxygen-containing functional groups, indicates that *B. vallismortis* might have produced more functional groups with a better degree of coordination.

The N1s spectra of Zn-EPS samples were fitted with four peaks while the control-EPS could only be fitted with two peaks (Fig. 5). In the N1s spectra of control-EPS, the peak at 399.8 eV represents amino nitrogen (R-NH₂/R₂-NH), while the peak at 401.3 eV indicates protonated nitrogen (R-NH₃⁺). The relative content of amino nitrogen of Zn-EPS was observed to decrease distinctly (Table 4). In addition, the peak observed at 403.0 eV was identified as quaternary ammonium (R₄-N⁺) and the peak at 405.0 eV represents nitril (–NO₂) [38]. Therefore, it could be speculated that amino groups were partially protonated under the induction of Zn and the appearance of nitril may be the result of nitrogen oxidation. The presence of heavy metals results in the generation of intracellular reactive oxygen species, which can potentially pass through the cell wall or remain extracellular, causing an external oxidizing environment, although this phenomenon requires further research.

The O1s peaks observed for both control-EPS and Zn-EPS, showed two peaks 531.2 and 532.5 eV (Table 5) which were assigned to O=C/C–OH and C–O, respectively [33, 36]. When comparing the two kinds of EPS,

Table 3 Analysis of XPS high-resolution C1s spectra of EPS produced by *B. vallismortis* in the presence or absence of Zn(II)

Peak	Binding energy(eV)	Atomic (%)		Assignments
		Control-EPS	Zn-EPS	
1	284.56–284.80	53.60	37.25	C–C/C–H
2	286.05–286.10	26.83	17.90	C–O/C–N
3	287.20	7.90	10.95	$\begin{matrix} \text{O} \\ \parallel \\ \text{—C—} \end{matrix} / \begin{matrix} \text{O} \\ \parallel \\ \text{—C—OH} \end{matrix}$
4	288.00–289.2	11.67	33.90	O–C–O/ $\begin{matrix} \text{O} \\ \parallel \\ \text{—C—NH} \end{matrix}$

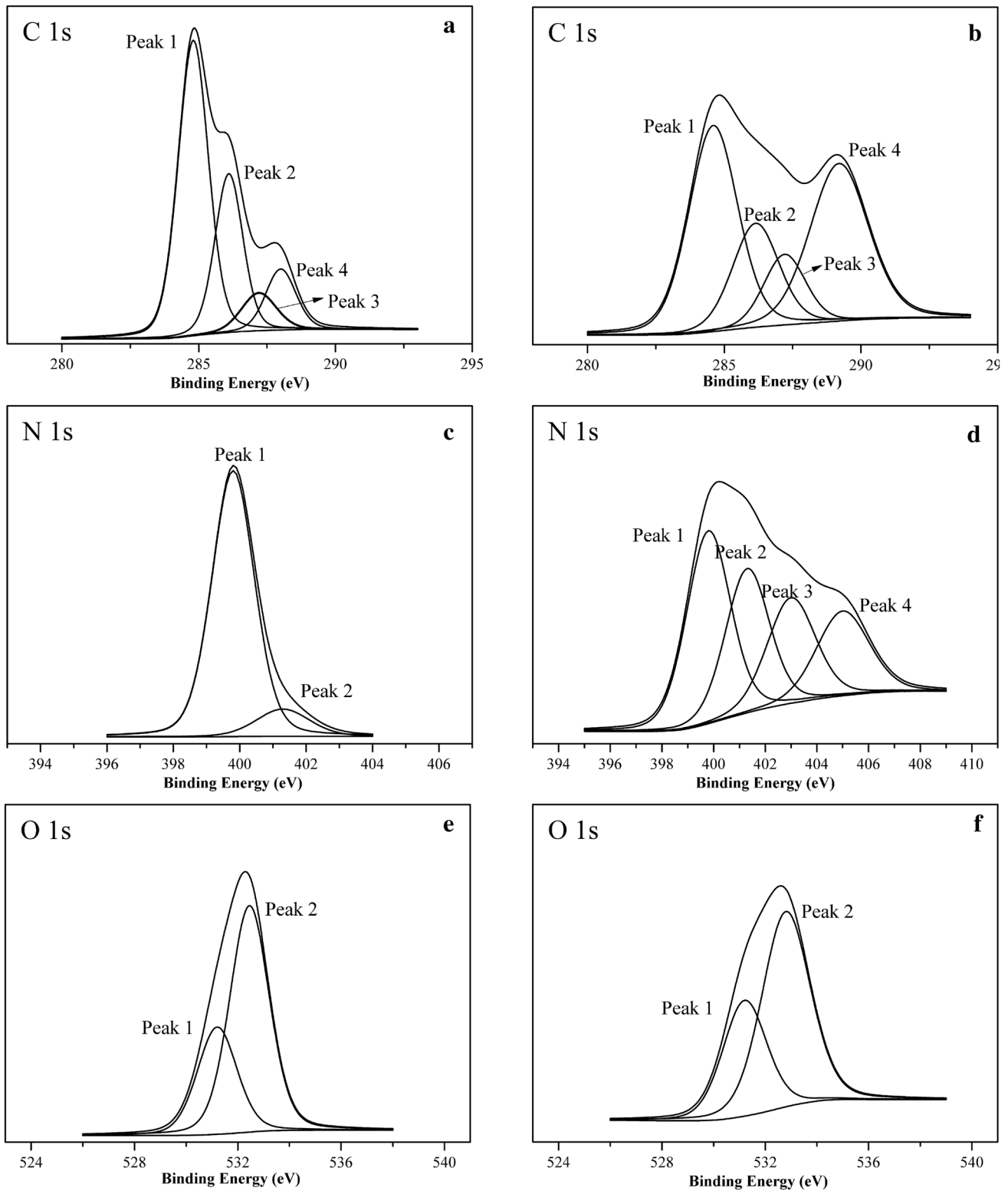


Fig. 5 XPS high-resolution C1s (a control-EPS, b Zn-EPS); N1s (c control-EPS, d Zn-EPS); and O1s (e control-EPS, f. Zn-EPS) spectra of EPS produced by *B. vallismortis* in the presence or absence of Zn(II)

Table 4 Analysis of XPS high-resolution N1s spectra of EPS produced by *B. vallismortis* in the presence or absence of Zn(II)

Peak	Binding energy (eV)	Atomic (%)		Assignments
		EPS	Zn-EPS	
1	399.8	88.59	34.77	R-NH ₂ /R ₂ -NH
2	401.3	11.41	26.00	R-NH ₃ ⁺
3	403.0	–	20.92	R ₄ -N ⁺
4	405.0	–	18.30	–NO ₂

Table 5 Analysis of XPS high-resolution O1s spectra of EPS produced by *B. vallismortis* in the presence or absence of Zn(II)

Peak	Binding energy (eV)	Atomic (%)			Assignments
		EPS	Zn-EPS	Cu-EPS	
1	531.2	32.13	35.04	39.76	C=O/C–OH
2	532.45–532.8	67.87	64.96	60.24	C–O

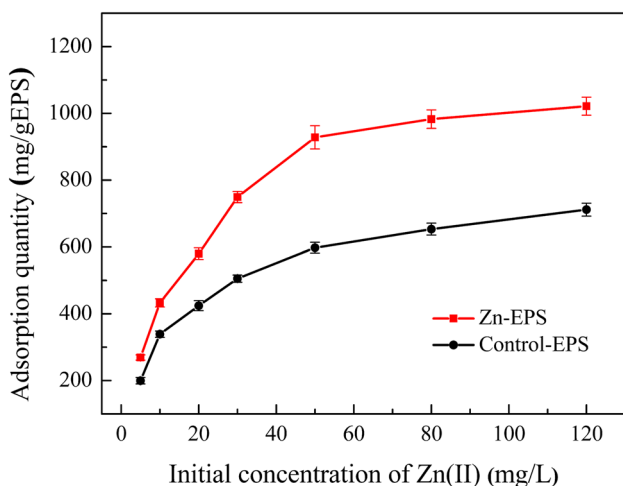


Fig. 6 Effect of initial concentration of Zn(II) on adsorption by EPS produced by *B. vallismortis* in the presence or absence of Zn(II)

the relative content of O=C/C–OH of Zn-EPS increased, while the relative contents of C–O decreased. This finding implies that a fraction of C–O was transformed to carbon double bonds or a hydroxyl group following Zn(II) stress,

helping to improve the ability of EPS to complex with metals.

Effect of initial Zn(II) concentration on adsorption quantity

Initial metal ion concentration of the solution is an important factor in determining the metal adsorption capacity of a biosorbent [39]. The effect of initial metal concentration on Zn(II) adsorption capacity of EPS produced by *B. vallismortis* in the presence or absence of Zn(II), is presented in Fig. 6. With increased initial metal ion concentrations from 5 to 50 mg L⁻¹, the Zn(II) adsorption capacity (mg g⁻¹ EPS) increased consistently in both EPS types. However, the adsorption capacity of Zn-EPS was notably higher than in control-EPS within the experimental range assessed in this paper.

Adsorption isotherms

To understand and compare the adsorption processes in both EPS types, Langmuir and Freundlich isotherms were applied to equilibrium data, with the fitted results depicted in Table 6. The higher R² value observed for both control- and Zn-EPS types, shows the better applicability of the Langmuir isotherm as compared to the Freundlich isotherm. The maximum adsorption capacity reflects the capacity of adsorbents to bind metal ions using the Langmuir isotherm. The equilibrium constant value is relative to the nature of the adsorbent and adsorbate, as well as the reaction temperature, with the adsorption ability being stronger when there is a high value of equilibrium. When comparing the two EPS types, the value of Q_e and b, representing adsorption capacity were found to be higher for Zn-EPS than control-EPS, indicating that Zn-EPS has a better affinity to Zn(II). Therefore, it may be surmised that the adsorption ability of Zn-EPS to Zn(II) was stronger due to specific EPS adaptations induced under the stress of Zn(II) exposure.

Table 6 Adsorption isotherm model information for EPS produced by *B. vallismortis* in the presence or absence of Zn(II)

EPS	Langmuir			Freundlich		
	Q _e (mg g ⁻¹)	b (L mg ⁻¹)	R ²	k (g L ⁻¹)	1/n	R ²
Control-EPS	750.92	0.116	0.996	185.69	0.303	0.960
Zn-EPS	1072.08	0.170	0.995	289.93	0.296	0.975

Conclusions

Both polysaccharides and protein were found to be influenced by the stress of Zn(II) exposure, with the variation in polysaccharides being larger. These findings indicate that *B. vallismortis* could produce specific extracellular polysaccharides in the presence of toxic metals as a defense mechanism, improving the adsorption capacity of EPS produced by *B. vallismortis*. The presence of Zn(II) stimulated the strain to produce specific EPS components, which protect the cell through isolating and immobilizing metal ions. Zn(II) exposure did not change the types of EPS functional groups present, but increased the relative abundance of surface functional groups.

Acknowledgements This work was supported by the Guangdong Provincial Science and Technology Planning Project (No.2014A020209077).

Compliance with ethical standards

Conflict of interest The authors declare that they have no conflict of interest.

References

- Nourbakhsh M, Sağ Y, Özer D, Aksu Z, Kutsal T, Çağlar A (1994) A comparative study of various biosorbents for removal of chromium(VI) ions from industrial waste waters. *Process Biochem* 29:1–5
- More TT, Yadav JS, Yan S, Tyagi RD, Surampalli RY (2014) Extracellular polymeric substances of bacteria and their potential environmental applications. *J Environ Manag* 144:1–25
- Sheng GP, Yu HQ, Li XY (2010) Extracellular polymeric substances (EPS) of microbial aggregates in biological wastewater treatment systems: a review. *Biotechnol Adv* 28:882
- Deschatre M, Ghillebaert F, Guezennec J, Colin CS (2013) Sorption of copper(II) and silver(I) by four bacterial exopolysaccharides. *Appl Biochem Biotechnol* 171:1313–1327
- Hou W, Ma Z, Sun L, Han M, Lu J, Li Z, Mohamad OA, Wei G (2013) Extracellular polymeric substances from copper-tolerance *Sinorhizobium meliloti* immobilize Cu²⁺. *J Hazard Mater* 261C:614–620
- Yue ZB, Li Q, Li CC, Chen TH, Wang J (2015) Component analysis and heavy metal adsorption ability of extracellular polymeric substances (EPS) from sulfate reducing bacteria. *Bioresour Technol* 194:399–402
- Chen B, Li F, Liu N, Ge F, Xiao H, Yang Y (2015) Role of extracellular polymeric substances from *Chlorella vulgaris* in the removal of ammonium and orthophosphate under the stress of cadmium. *Bioresour Technol* 190:299–306
- Cheng YJ, SONG WF, LIN LT, DONG M (2016) Anaerobic biodegradation and mechanism of aniline aerofloat. *China Environ Sci* 4:033–038
- Raunkjær K, Hvitved-Jacobsen T, Nielsen PH (1994) Measurement of pools of protein, carbohydrate and lipid in domestic wastewater. *Water Res* 28:251–262
- Bradford MM (1976) A rapid and sensitive method for the quantitation of microgram quantities of protein utilizing the principle of protein–dye binding. *Anal Biochem* 72:248–254
- Sun Y, Clinkenbeard KD, Clarke C, Cudd L, Highlander SK, Dabo SM (1999) Pasteurella haemolytica leukotoxin induced apoptosis of bovine lymphocytes involves DNA fragmentation. *Vet Microbiol* 65:153–166
- Raliya R, Tarafdar JC, Mahawar H, Kumar R, Gupta P, Mathur T, Kaul RK, PraveenKumar, Kalia A, Gautam R (2014) ZnO nanoparticles induced exopolysaccharide production by *B. subtilis* strain JCT1 for arid soil applications. *Int J Biol Macromol* 65:362
- Ueshima M, Ginn BR, Haack EA, Szymanowski JES, Fein JB (2008) Cd adsorption onto *Pseudomonas putida* in the presence and absence of extracellular polymeric substances. *Geochim Cosmochim Acta* 72:5885–5895
- Graż M, Pawlikowska-Pawłęga B, Jarosz-Wilkolazka A (2011) Growth inhibition and intracellular distribution of Pb ions by the white-rot fungus *Abortiporus biennis*. *Int Biodeter Biodegrad* 65:124–129
- Chen A, Shang C, Zeng G, Chen G, Shao J, Zhang J, Huang H (2015) Extracellular secretions of *Phanerochaete chrysosporium* on Cd toxicity. *Int Biodeter Biodegrad* 105:73–79
- Chen A, Zeng G, Chen G, Liu L, Shang C, Hu X, Lu L, Chen M, Zhou Y, Zhang Q (2014) Plasma membrane behavior, oxidative damage, and defense mechanism in *Phanerochaete chrysosporium* under cadmium stress. *Process Biochem* 49:589–598
- Kim SH, Kim SK, Jung KH, Kim YK, Hwang HC, Ryu SG, Chai YG (2013) Proteomic analysis of the oxidative stress response induced by low-dose hydrogen peroxide in *Bacillus anthracis*. *J Microbiol Biotechnol* 23:750–758
- Wan J, Zeng G, Huang D, Huang C, Lai C, Li N, Wei Z, Xu P, He X, Lai M (2015) The oxidative stress of phanerochaete chrysosporium against lead toxicity. *Appl Biochem Biotech* 175:1981–1991
- Naik MM, Pandey A, Dubey SK (2012) Biological characterization of lead-enhanced exopolysaccharide produced by a lead resistant *Enterobacter cloacae* strain P2B. *Biodegradation* 23:775–783
- Coble PG (1996) Characterization of marine and terrestrial DOM in seawater using excitation-emission matrix spectroscopy. *Mar Chem* 51:325–346
- Chen W, Westerhoff P, Leenheer JA, Booksh K (2003) Fluorescence excitation-emission matrix regional integration to quantify spectra for dissolved organic matter. *Environ Sci Technol* 37:5701–5710
- Stedmon CA, Markager S, Bro R (2003) Tracing dissolved organic matter in aquatic environments using a new approach to fluorescence spectroscopy. *Mar Chem* 82:239–254
- Guo XJ, He LS, Li Q, Yuan DH, Deng Y (2014) Investigating the spatial variability of dissolved organic matter quantity and composition in Lake Wuliangshuai. *Ecol Eng* 62:93–101
- Wu F, Tanoue E (2001) Isolation and partial characterization of dissolved copper-complexing ligands in streamwaters. *Environ Sci Technol* 35:3646
- Wang J, Li Q, Li MM, Chen TH, Zhou YF, Yue ZB (2014) Competitive adsorption of heavy metal by extracellular polymeric substances (EPS) extracted from sulfate reducing bacteria. *Bioresour Technol* 163:374–376
- Wang Z, Gao M, Wang Z, She Z, Chang Q, Sun C, Zhang J, Ren Y, Yang N (2013) Effect of salinity on extracellular polymeric substances of activated sludge from an anoxic–aerobic sequencing batch reactor. *Chemosphere* 93:2789–2795
- Wang ZW, Wu ZC, Tang SJ (2009) Characterization of dissolved organic matter in a submerged membrane bioreactor by using three-dimensional excitation and emission matrix fluorescence spectroscopy. *Water Res* 43:1533–1540

28. Yin Y, Hu Y, Xiong F (2011) Sorption of Cu(II) and Cd(II) by extracellular polymeric substances (EPS) from *Aspergillus fumigatus*. *Int Biodeter Biodegrad* 65:1012–1018
29. Fang L, Wei X, Cai P, Huang Q, Chen H, Liang W, Rong X (2011) Role of extracellular polymeric substances in Cu(II) adsorption on *Bacillus subtilis* and *Pseudomonas putida*. *Biores Technol* 102:1137–1141
30. Jiang W, Saxena A, Song B, Ward BB, Beveridge TJ, Myneni SC (2004) Elucidation of functional groups on gram-positive and gram-negative bacterial surfaces using infrared spectroscopy. *Langmuir ACS J Surf Colloids* 20:11433–11442
31. Xu Y, Hou M, Ruan J, Qu M, Sun H, Xu J, Zhou S (2014) Effect of magnetic field on surface properties of CrA and its extracellular polymeric substances (EPS). *J Adhes Sci Technol* 28:2196–2208
32. Badireddy AR, Chellam S, Gassman PL, Engelhard MH, Lea AS, Rosso KM (2010) Role of extracellular polymeric substances in bioflocculation of activated sludge microorganisms under glucose-controlled conditions. *Water Res* 44:4505–4516
33. Lin D, Ma W, Jin Z, Wang Y, Huang Q, Cai P (2015) Interactions of EPS with soil minerals: a combination study by ITC and CLSM. *Colloids Surf B Biointerfaces* 138:10–16
34. Rouxhet PG, Mozes N, Dengis PB, Dufrêne YF, Gerin PA, Genet MJ (1994) Application of X-ray photoelectron spectroscopy to microorganisms. *Colloids Surf B Biointerfaces* 2:347–369
35. Yang Y, Wikieł AJ, Dall'Agnol LT, Eloy P, Genet MJ, Moura JJ, Sand W, Dupont-Gillain CC, Rouxhet PG (2016) Proteins dominate in the surface layers formed on materials exposed to extracellular polymeric substances from bacterial cultures. *Biofouling* 32:95–108
36. Li Y, Li Q, Fengying Y, Bao J, Hu Z, Zhu W, Zhao Y, Lin Z, Dong Q (2015) Chromium (VI) detoxification by oxidation and flocculation of exopolysaccharides from *Arthrobacter* sp. B4. *Int J Biol Macromol* 81:235–240
37. Bautista BET, Wikieł AJ, Datsenko I, Vera M, Sand W, Seyeux A, Zanna S, Frateur I, Marcus P (2014) Influence of extracellular polymeric substances (EPS) from *Pseudomonas* NCIMB 2021 on the corrosion behaviour of 70Cu–30Ni alloy in seawater. *J Electroanal Chem* 737:184–197
38. Szcześ A, Czemińska M, Jarosz-Wilkolazka A (2016) Calcium carbonate formation on mica supported extracellular polymeric substance produced by *Rhodococcus opacus*. *J Solid State Chem* 242:212–221
39. Sharma M, Kaushik A, Somvir, Bala K, Kamra A (2008) Sequestration of chromium by exopolysaccharides of *Nostoc* and *Gloeocapsa* from dilute aqueous solutions. *J Hazard Mater* 157:315–318